Proceedings World Geothermal Congress 2020+1
Reykjavik, Iceland, April - October 2021

Silica Nanoparticles Produced by Flash Vaporization from Supercritical Fluids

Atsushi Okamoto[1], Takamasa Niibe[1], Takashi Amagai[1,2], Nobuo Hirano[1] and Noriyoshi Tsuchiya[1]

[1]Graduate School of Environmental Studies, Tohoku University, Aoba 6-6-20, Aramaki, Aoba-ku Sendai, 980-8579, Japan

[2]Japan Oil, Gas and Metals National Corporation, 10-1, Toranomon 2-chome, Minato-ku, Tokyo, 105-0001 Japan

E-mail address, atsushi.okamoto.d4@tohoku.ac.jp

Keywords: Silica, Nanoparticles, Flash vaporization, Supercritical fluids

ABSTRACT

The knowledge of water-rock interaction at high temperature is crucial for understanding the effective power generation from supercritical geothermal reservoirs. In particular, the characteristics and behaviors of silica in super-heated steam are still poorly understood. In this study, we conducted flash experiments of high-silica solutions from sub to supercritical conditions (~350 ˚C and ~450 ˚C at ~36 MPa) and the products caught by the alumina filter were investigated in detail. The input solutions were prepared by dissolution of sands of granite, quartz and basalt in distilled water at subcritical conditions. The flash experiments showed nearly isothermal decompression, and phase changes of water occurred within 1 second. In all cases, we found the formation of spherical particles of amorphous silica that was 100 nm to 10 μm in size. In the experiments with basalt-dissolved solutions, micron-scale elongated crystals (probably albite) were also found. Our results suggest that the transport, growth and adhesion behavior of such nano to micron-scale particles plays an important role in the clogging of fractures and mineral scaling.

1. INTRODUCTION

Recently, supercritical or superhot geothermal reservoirs have received much attention as a frontier of renewable energy, and the drilling projects into hotter parts of hydrothermal systems have been conducted around the world including Iceland, Italy and Japan (e.g., Doi et al., 1998; Friðleifsson et al., 2017; Reinsch et al., 2017; Kruszewski et al., 2018). However, our knowledge of the nature of water-rock interaction at such high temperatures is still limited. Silica scaling is a particularly serious problem as it reduces the efficiency of power generation. Although it is expected that a large amount of silica could be contained in fluids or steam from the supercritical reservoirs, few studies have been conducted on the formation of silica scaling at high temperatures (>300 ˚C; Karlsdottir et al., 2015).

The solubility of silica minerals such as quartz and amorphous silica in water varies as a function of temperature and water density (Fig. 1a; e.g., Fournier and Potter, 1982; Manning, 1994; Akinsief and Diamond, 2009; Karásek et al., 2013). In geothermal areas with high geothermal gradient, drastic change in water density occurs with depth, and thus the dissolution and precipitation of silica minerals plays an important role in shaping and maintaining the productivity of geothermal reservoirs (Fournier, 1991; 1998; Saishu et al., 2014; Tsuchiya, et al. 2016; Okamoto et al., 2017). One of the plausible mechanisms of silica precipitation is decompression of fluids (e.g., Rusk and Reed, 2002). Deep within hydrothermal systems, fluid pressure can fluctuate between lithostatic and hydrostatic induced by seismic events, which causes silica supersaturation. Recently, a drastic scenario for quartz-gold veins has been proposed by Weatherley and Henley (2013). In their model, at the instance of earthquake, the fluid pressure drops at the fault jog below hydrostatic pressure (up to vapor), and such flash vaporization could cause co-precipitation of silica and gold. The situation of flash vaporization is similar to the situation of the production well of the geothermal systems. Karlsdottir et al. (2015) conducted the in situ test of IDDP-1 site of Island at 350 ˚C and revealed a rapid growth of silica scaling. It is expected that superheated steam produced from the supercritical reservoir contains a large concentration of silica, but the nature of silica in high-temperature steam is not clarified. The kinetics of silica precipitation has been mainly investigated based on surface reactions of preexisting minerals (Rimstidt and Barnes, 1980), and therefore, mechanism and rate of silica precipitation at extremely high-supersaturated conditions are poorly understood.

Our research group has conducted a series of silica precipitation experiments at supercritical conditions (c.a. 430 ˚C, 30 MPa) using a flow-through apparatus (Okamoto et al., 2010; Okamoto and Sekine, 2011; Saishu et al., 2012; Saishu et al., 2014). These experiments revealed that depending on P-T conditions, solution chemistry (supersaturation, trace elements such as Na and Al) and type of rock substrates, silica precipitation occurs in various ways including epitaxial growth of pre-existing quartz grains, homogeneous or heterogeneous nucleation of quartz and formation of metastable silica minerals, such as amorphous silica, cristobarite (opal-C), and chalcedony. Recently, we have conducted a new type of silica precipitation by flashing of granite-dissolved aqueous solutions from sub- to supercritical conditions (Amagai et al., 2019), and reported that amorphous silica was produced induced by flash vaporization. In this contribution, based on the data of Amagai et al. (2019) and of additional flash experiments with using different input solutions (Fig. 1b), we reveal that characteristics of precipitates produced by flash vaporization, and discuss the implications to the developments on the supercritical geothermal reservoirs.

2. EXPERIMENTAL METHOD

2.1 Apparatus

We used the main autoclave (110 ml) where the inner wall and inner caps were made of a titanium alloy (64 Ti) and titanium, respectively (Fig. 2). The autoclave was placed vertically in the furnace and was connected to a water tank, syringe pump, stop valve, and back pressure valve by the stainless-steel pipes (SUS316). Temperature was measured at the center of the autoclave and fluid pressure was measured at the inlet. For catching the silica precipitates, we installed a cylindrical alumina filter (Fuji Chemical, FA220, diameter of 6.3 mm, height of 5.0 mm, average pore diameter, ~60 μm) within the outlet inner cap.

2.2 Experiments and analyses

We prepared three types of the input solution of the flash experiments by dissolution of sands of granite (Amagai et al., 2019), quartz, and basalt from Iceland. Distilled water entered the cylindrical flow-through autoclave at a constant flow rate of 0.5-1.0 ml/min, and the sands of granite, quartz and basalt were dissolved at 360-370 ˚C and 35-41 MPa, and the solutions were stored in water tank. Table 1 shows the concentrations of Si, Al, Fe, Mg, Ca, Na and K of the input solutions measured were determined by inductively coupled plasma–atomic emission spectrometry (ICP–AES, HITACHI P-4000) at Tohoku University, Sendai, Japan. The concentrations of Si in the quartz-dissolved (273.8 mg/kgH_2O) and granite-dissolved solutions (258.3 mg/kgH_2O) are similar to each other, whereas Si concentration in the basalt-dissolved solution was relatively low (172.5 mg/kgH_2O). Al (17.2 mg/kgH_2O) and Na (39.9 mg/kgH_2O) concentrations in the basalt-dissolved solution are higher than those in the granite-dissolved solution (Al = 5.9 mg/kgH_2O, Na = 6.8 mg/kgH_2O). The concentrations of K and Ca are similar between granite-dissolved and basalt-dissolved solutions.

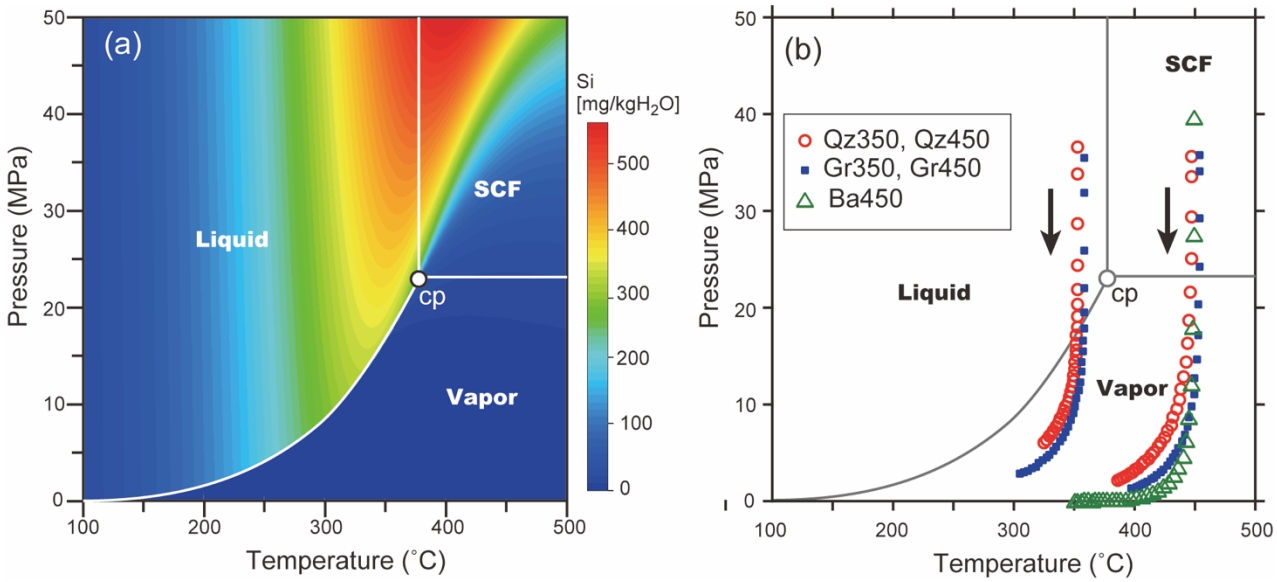

Figure 1: (a) The solubility of quartz in water (Si, mg/kgH_2O) in the phase diagram of water calculated following Manning (1994). (b) The P-T paths of the flash experiments (within 3 seconds after flashing) using the quartz-dissolved solution at ~350 ˚C and ~450 ˚C (Qz350, Qz450), granite-dissolved solution at ~350˚C and ~450 ˚C (Gr350, Gr450) and basalt-dissolved solution at ~450 ˚C (Ba450). P-T conditions were recorded in 0.1 second interval. SCF = supercritical fluid. Cp = critical point of water.

Table 1: The compositions of starting solutions used for the flash experiments.

	Si	Al	Fe	Mg	Ca	Na	K	pH*
				mg/kgH_2O				
Qtz-dissolved solution	273.8	n.a.	n.a.	n.a.	n.a.	n.a.	n.a.	n.a
Granite-dissolved solution	258.4	5.9	<0.1	<0.1	1.9	6.8	6.1	6.8
Basalt-dissolved solution	172.5	17.2	<0.1	<0.1	1.1	39.9	5.2	7.9
*pH at room temperature								
n.a. = not analyzed.								

Before the flash experiments, the autoclave was filled with the starting solution (Table 1) using the syringe pump at room temperature. Then, the solution was pressurized to ~36 MPa by controlling the back-pressure valve. At the time of flashing, the fluid pressure instantaneously dropped to the atmospheric pressure by opening the stop valve; due to the volume increase by decompression, a large amount of upward fluid flow occurred through the alumina filter, which caught the particles of silica precipitates. We conducted a series of the flashing from the subcritical condition ~36 MPa and ~350 ˚C (Qz350; Gr350), and the

supercritical condition 450 ˚C (Qz450; Fr450; Ba450), respectively. The changes of P-T condition were recorded in the data logger with time intervals of 0.1s. After the flashing experiments, we took the alumina filter, and observed silica precipitates on it using the Field Emission Scanning Electron Microscope (FESEM, HITACHI SU-8000) at Tohoku University. Silica minerals were identified using a micro-Raman spectroscope (HORIBA XploRA PLUS) at Tohoku University equipped with a 532 nm laser and 2400 grooves/mm grating, as possible.

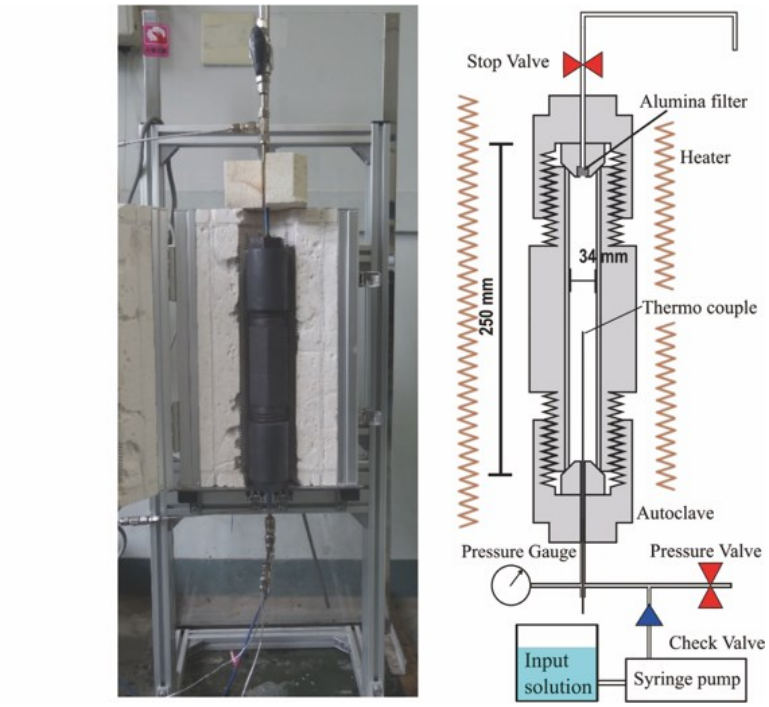

Figure 2: Photo (left) and schematic illustration (right) of experimental apparatus of flash experiments.

3. RESULTS AND DISCUSSION

Figure 1b shows the P-T paths within 3 seconds after the flashing in all runs. All the runs showed almost isothermal decompression with pressures to below 5 MPa, and water changed from liquid to vapor at 350 ˚C and from supercritical fluids to vapor at 450 ˚C within 1 second to produce superheated steam. In a duration of 1-3 seconds, the temperature slightly decreased probably due to the evaporation of liquid water in the capillary tube.

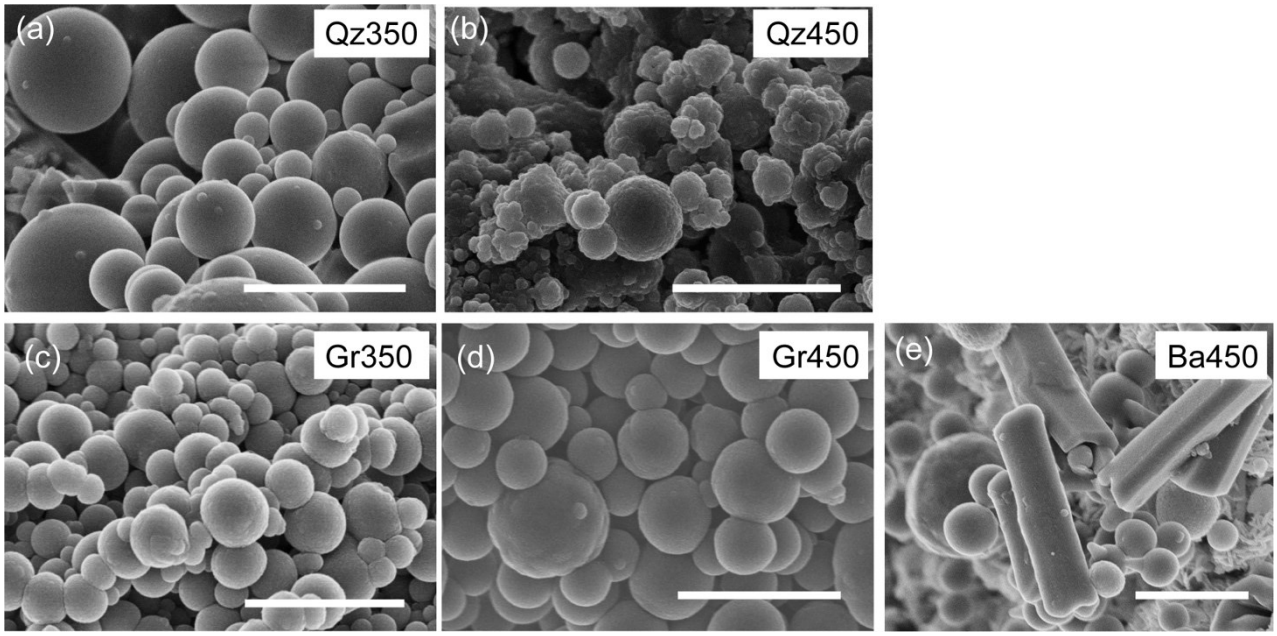

Figure 3: The SEM photos of the surface morphologies of the products produced by flash experiments. (a) quartz-dissolved solution at 350 ˚C (Qz350), (b) quartz-dissolved solution at 450 ˚C (Qz450), (c) granite-dissolved solution at 350 ˚C (Gr350), (d) granite-dissolved solution at 450 ˚C (Gr450), and (e) basalt-dissolved solution at 450 ˚C (Ba450). Gr350 and Gr450 were taken from the results of Amagai et al., (2019). Scale bars indicate 2 μm.

Figure 3 shows the SEM photos of the products of the flash experiments. The products from the quartz-dissolved solution (Qz350, Qz450; Fig. 3a, b) and from the granite-dissolved solution (Gr350, Gr450; Fig. 3c, d) showed the similar characteristic features. On the alumina filter, the spherical particles with sizes of ~100 nm to 6 μm were collided and stacked on the alumina filter. Raman spectroscopy revealed that these particles are amorphous silica, and semiquantitative EDS analyses showed that <1 wt% of Al_2O_3 and K_2O, and 1-2 wt% of Na_2O were contained in the products from the granite-dissolved solution (Amagai et al., 2019). There are no systematic differences in size and shapes in the particles between 350 and 450 ˚C (Fig. 3a-d), but the amount of the precipitates on alumina filter at the 350 ˚C seems smaller than those at 450 ˚C. As the solubility of silica minerals in vapor is low at both 350 and 450 ˚C, the difference of the precipitation amounts could suggest that smaller silica particles (<100 nm) passed though the alumina filter at 350 ˚C. Some of the silica particles show the cauliflower-like surface morphology with wavelength of 100-200 nm (Fig. 3a-d), suggesting that these silica particles were probably produced not only by homogeneous nucleation but also aggregation during the evaporation of droplets.

Quartz is the most stable silica phase in crusts, whereas the flashing products are amorphous silica. However, the flashing causes the drastic changes of water density, leading to a supersaturation ratio of not only quartz but also amorphous silica. As the surface energy of amorphous silica (65 mJ m^{-2}) with respect to water is lower than that of quartz (350 mj m^{-2}; Lasaga, 1998; Amagai et al., 2019), amorphous silica firstly nucleated from the solutions. When these amorphous silica particles were put in hydrothermal solutions, they rapidly changed to more stable phases (cristobalite and quartz) by heterogeneous nucleation and dissolution-precipitation processes (Okamoto et al., 2015; Amagai et al., 2019).

In contrast to the flash experiments with the quartz and granite-dissolved solutions, the experiments with the basalt-dissolved solution produced the elongated crystals with 3-5 μm in length and ~1 μm in width, as well as the spherical amorphous particles in similar size of the other experiments (Fig. 3e). Although it is difficult to identify these crystals by Raman spectroscopy due to the background of the alumina filter, they are probably albite considering the Na and Al-rich solution chemistry (Table 1) and crystal shape (Fig. 3e). Therefore, the results of this study (Fig. 3) suggested that the granite and basalt-hosted geothermal systems produced the different types of scale. However, it is noted that the chemical compositions of the basalt-dissolved solution in this study is different from those of geothermal fluids in IDDP-1 and 2 sites, as (1) IDDP-1 encounters the rhyolite magma meaning that it is not pure basalt-water interaction (Elders et al., 2015), and (2) IDDP-2 sites are characterized by an infiltration of seawater (Friðleifsson et al., 2017), where the Na-rich composition of seawater could prevent the dissolution of albite from plagioclase.

This study indicates that superheated steam produced from the supercritical or superhot geothermal reservoirs contains nano to micron-scale particles of silica minerals. Further investigations for dynamic behavior of these particles are required for flow, aggregation and adhesion processes for understanding their effects on the permeability of the reservoirs and for reducing the scaling and corrosion of pipelines as well as turbines during the operation of geothermal power plants.

ACKNOWLEDGEMENTS

A.O. and N.T. received support through JSPS KAKENHI Grant Numbers 16H06347, 17H02981 and 25000009, respectively. This paper is partly based on results obtained from a project commissioned by the New Energy and Industrial Technology Development Organization (NEDO).

REFERENCES

Amagai, T., Okamoto, A., Niibe, N., Hirano, N., Motomiya, K., and Tsuchiya, N.: Silica nanoparticles produced by explosive flash vaporization during earthquakes. Scientific Reports, **9**, (2019), 9738.

Akinfiev, N.N., and Diamond, L.W.A.: simple predictive model of quartz solubility in water–salt–CO2 systems at temperatures up to 1000 ˚C and pressures up to 1000 MPa. *Geochimica et Cosmochimica Acta*, **73**, (2009), 1597–1608.

Doi, N., Kato, O., Ikeuchi, K., Komatsu, R., Miyazaki, S., Akaku, K., Uchida, T., 1998. Genesis of the plutonic-hydrothermal system around quaternary granite in the Kakkonda geothermal system, Japan. Geothermics 27, 663-690.

Elders, W.A., Friðleifsson, G.Ó., Zierenberg, R.A., Pope, E.C., Mortensen, A.K., Guðmundsson, Á., Lowenstern, J.B., Marks, N.E., Owens, L., Bird, D.K., Reed, M., Olsen, N.J., and Schiffman, P.: Origin of a rhyolite that intruded a geothermal well while drilling at the Krafl a volcano, Iceland. *Geology*, **39**, (2011), 231-234.

Fournier, R.O., and Potter, II, R.W.: An equation correlating the solubility of quartz in water from 25 ˚C to 900 ˚C at pressures up to 10,000 bars. *Geochimica et Cosmochimica Acta* **46**, (1982), 1969–1973.

Fournier, R.O.: The transition from hydrostatic to greater than hydrostatic fluid pressure in presently active continental hydrothermal systems in crystalline rock. *Geophysical Research Letters*, **18**, 955–958 (1991).

Fournier, R.O.: Hydrothermal processes related to movement of fluid from plastic into brittle rock in the magmatic–epithermal environment. *Economic Geology*, **94**, (1999), 1193–1211.

Friðleifsson, G.Ó., Elders, W.A., Zierenberg, R.A., Stefánsson, A., Fowler, A.P.G., Weisenberger, T.B., Harðarson, B.S., and Mesfin, K.G.: The Iceland Deep Drilling Project 4.5km deep well, IDDP-2, in the seawater-recharged Reykjanes geothermal field in SW Iceland has successfully reached its supercritical target, *Scientific Drilling*, **23**, (2017), 1-12.

Karasek, P., and Šťavíková, L., Planeta, J., Hohnová, B., and Roth, M.: Solubility of fused silica in sub- and supercritical water: Estimation from a thermodynamic model. *The Journal of Supercritical Fluids*, **83**, (2013), 72–77.

Karlsdottir, S.N., Rangnarsdottir, K.R., Thorbjornsson, I.O., Einarsson, A.: Corrosion testing in superheated geothermal steam in Iceland. *Geothermics*, **53**, (2015), 281-290.

Kruszewski, M., and Wittig, V., Review of failure modes in supercritical geothermal drilling projects. *Geothermal Energy*, **6**, (2018), 28.

Manning, C.E.: The solubility of quartz in H2O in the lower crust and upper mantle. *Geochimica et Cosmochimica Acta*, **58**, (1994), 4831–4839.

Okamoto, A., Saishu, H., Hirano, N. and Tsuchiya, N.: Mineralogical textural variation in hydrothermal flow-through experiments: implications for quartz vein formation. Geochimica et Cosmochimica Acta **74**, (2010), 3692–3706.

Okamoto, A., and Sekine, K.: Texture of syntaxial quartz veins synthesized by hydrothermal experiments. Journal of Structural *Geology*, **33**, (2011), 1764–1775.

Okamoto, A., Kuwatani, T., Omori, T., Hukushima, K.: Free-energy landscape and nucleation pathway of polymorphic minerals from solution in a Potts lattice-gas model. Physical Review E, 92, (2015), 042130, DOI: 10.1103/PhysRevE.92.042130.

Okamoto, A., Tanaka, H., Watanabe, N., Saishu, H., Tsuchiya, N., Fluid pocket generation in response to heterogeneous reactivity of a rock fracture under hydrothermal conditions. Geophysical Research Letters, 44, (2017), doi.org/10.1002/2017GL075476.

Reinsch, T., Dobson, P., Asanuma, H., Huenges, E., Poletto, F., and Sanjuan, B.: Utilizing supercritical geothermal systems: a review of past ventures and ongoing research activities. *Geothermal Energy*, **5**, (2017), 16.

Rimstidt, J.D., and Barnes, H.L.: The kinetics of silica–water reactions. Geochimica et Cosmochimica Acta 44, 1683–1699 (1980).

Rusk, B., and Reed, M.: Scanning electron microscope–cathodoluminescence analysis of quartz reveals complex growth histories in veins from the Butte porphyry copper deposit, Montana. *Geology*, **30**, 727–730 (2002).

Saishu, H., Okamoto, A. & Tsuchiya, N. Mineralogical variation of silica induced by Al and Na in hydrothermal solutions. *American, Mineralogist*, **97**, (2012), 2060–2063.

Saishu, H., Okamoto, A., and Tsuchiya, N.: The significance of silica precipitation on the formation of the permeable–impermeable boundary within Earth's crust. Terra Nova, **26**, 253–259 (2014).

Tsuchiya, N., Yamada, R., Uno, M., Supercritical geothermal reservoir revealed by a granite-porphyry system. *Geothermics*, **63**, (2016), 182-194.

Weatherley, D.K., Henley, R.W.: Flash vaporization during earthquakes evidenced by gold deposits. *Nature Geoscience*, **6**, (2013), 294..